applied sciences

MDPI

Article

Non-Destructive Infrared Evaluation of Thermo-Physical Parameters in Bamboo Specimens

Juan Felipe Florez-Ospina *, Juan Esteban Ospina-Borras and Hernán Darío Benitez-Restrepo

Department of Electronics and Computer Science, Pontificia Universidad Javeriana Cali, Cali 760031, Colombia; ospina.juanesteban@gmail.com (J.E.O.-B.); benitez@ieee.org (H.D.B.-R.)

* Correspondence: juanflo16@gmail.com; Tel.: +1-302-333-9262

Received: 1 November 2017; Accepted: 27 November 2017; Published: 2 December 2017

Abstract: The estimation of heat conduction properties has considerable importance in the characterization of bamboo with respect to its potential use as an alternative construction material. Even though traditional methods such as hot plates have successfully measured thermal parameters, like thermal diffusivity and conductivity in bamboo samples, it is still necessary to transform the cylindrical bamboo specimen into a piece with special geometry and size. This requirement makes this method impractical in applications where several bamboo specimens need to be measured in their original cylindrical shape. This paper presents the estimation of thermo-physical parameters k and ρc_p in Guadua angustifolia kunth (Guadua a.k.) bamboo through nonlinear least square optimization and infrared thermography. A sensitivity analysis was carried out to determine how the temperature on the bamboo surface is affected by changes in the convection coefficient h, thermal conductivity k, and volumetric heat capacity ρc_p. In spite of the nonlinearity and high correlation in the parameters of the inverse heat conduction problem (IHCP), the estimation of such parameters is robust and consistent with those reported in the literature.

Keywords: inverse heat conduction problem; infrared thermography; thermo-physical properties; heat transfer coefficient; Guadua a.k.

1. Introduction

Some properties make bamboo an excellent construction material; three of them are its high specific strength, fast growth, and abundance. Bamboo is stronger and denser than North American softwoods like pine, fir, and spruce. In the last years, these reasons have promoted an increment in the use of bamboo for construction in some Latin-American and Asian countries [1].

Guadua angustifolia kunth (Guadua a.k.) is a giant species of bamboo that not only grows fast, reaching its maximum strength after 3–4 years, but also decreases greenhouse effects, capturing 40 times more CO_2 than pine trees. The beneficial mechanical properties mentioned above, along with its ability to absorb CO_2, turns Guadua a.k. into an interesting construction material for sustainable development and an alternative to concrete and steel [2].

Previous works on bamboo characterization have concentrated their efforts on measuring its mechanical and thermal properties. In [3], authors have measured mechanical properties such as flexural properties and compressive strengths in bamboo culms of a commercial species in China named Moso. Compared to common North American construction woods loaded along the axial direction, Moso bamboo is approximately as stiff and substantially stronger in both flexure and compression, but denser. Additionally, the experimental results of mechanical characterization in glued laminated Guadua a.k. reveals higher strength and comparable stiffness compared to those of engineered timbers commonly used in the United States [4,5]. The analysis of mechanical properties in bamboo species Kao Jue and Mao Jue usually used in Hong Kong and Southern China concluded that

they are good construction materials with excellent mechanical properties against compression and bending [6].

In addition to the measurement of mechanical properties in bamboo samples, previous bamboo characterizations have also been oriented toward the estimation of thermal parameters. One approach evaluated the insulating properties of the PLA (poly lactic acid) bamboo fiber 'green' composites by determination of the thermal conductivity, which was measured using a hot-wire method. The thermal conductivity of PLA-bamboo fiber 'green' composites was significantly influenced by their density [7]. Another approach, instead characterizes thermal conductivity of bamboo fiber reinforced polyester composite using a guarded heat flow meter method [8]. The results of this study indicated that the developed composite is an insulating material. In [9], the authors evaluated the thermal conductivity of bamboo mat board (BMB) based on a steady-state guarded hot-plate method, and studied the effect of density on thermal conductivity of BMB. In [10], based on a photoacoustic technique in frequency configuration, Gordillo et al. evaluated the thermophysical parameters of Guadua a.k. specimens such as thermal effusivity, thermal diffusivity, and thermal conductivity. The main findings show that thermal diffusivity is lower in the external region close to the bark surface, while this is kept constant along the stem.

Even though these approaches successfully measure bamboo thermal properties, these parameters are not uniform in the same sample, and it is necessary to convert the cylindrical bamboo culm into a sample with specific dimensions and shape. This need for adaption renders these methods impractical when testing numerous specimens whose geometries are mostly cylindrical. Hence, it is important to analyze non-invasive methods that permit the estimation of thermal parameters in bamboo samples.

Infrared thermography (IT) is a non-destructive technique that employs the heat emitted by bodies/objects to rapidly and noninvasively detect defects in specimens or estimate thermophysical parameters in materials [11,12]. In active IT, it is necessary to apply heat to the specimen inspected in order to obtain significant temperature differences that prove the presence of anomalies. In wood inspection, active IT has important applications such as the estimation of wood density [13], the imaging of moisture content distribution [14–16] and the detection of adhesion defects in laminated wood composites [17]. In bamboo inspection, active IT studied the glue interface between bamboo laminate, since it affects bamboo flooring quality. The researchers used active thermography using frequency modulated wave imaging (FMTW) and discovered glue deficiencies of gaps between laminates at different frequencies [18]. In spite of these applications of active IT in wood and bamboo inspection, to the extent of our knowledge, there are no previous works in inversion algorithms for the estimation of thermal parameters in bamboo cylindrical specimens. Nonetheless, active IT and inversion algorithms have provided good results in scenarios such as defect parameter estimation in composites [19], determination of material properties [20], and heat flux estimation [21].

In this work, we conduct the non-destructive estimation of Guadua a.k. thermal parameter k and ρc_p based on the inversion of infrared thermography data. This inversion method inspects the specimen in its cylindrical shape based on the discretization of a 1D direct heat transfer model in cylindrical coordinates. In spite of the importance of chemical preservation in Guadua a.k. to decrease its vulnerability to insect attacks, few studies have analyzed the effects of preservation on the thermal properties. In this paper, we compare the estimated values of k and ρc_p obtained from preserved and non-preserved specimens to observe how preservation impacts these parameters. The main contributions of this work are: (i) the estimation of thermal parameters k and ρc_p in Guadua a.k. through nonlinear least squares and infrared thermography; and (ii) the sensitivity analysis of the direct model with respect to thermal parameters k, ρc_p, h, and r. The remainder of this article is organized as follows: Sections 2 and 3 describe the theoretical thermal model and inverse problem formulation. Sections 4 and 5 introduce the estimation of thermal parameters in the presence of additive Gaussian noise and the experimental set-up. Finally, Sections 6 and 7 estimate the thermal parameters in bamboo specimens and conclude the paper.

2. Theoretical Model

For this research, we use the Cepa of the Guadua a.k, which corresponds to the lowest part of the trunk. The wall thickness and outside diameter of Cepa provide appropriate strength for its use in construction [22]. Cepa geometry can be properly described with cylindrical coordinates. Therefore, in this section, we present the theoretical model of the radial heat transfer in a cylinder heated from inside to a temperature $T_s(t)$ and subjected to convective heat loss. This phenomenon is formulated in Equation (1).

$$\frac{1}{r}\frac{\partial}{\partial r}\left(rk\frac{\partial T}{\partial r}\right) = \rho c_p \frac{\partial T}{\partial t} \quad \text{in } r_0 < r < R, \quad \text{for } t > 0, \tag{1a}$$

$$T = T_s(t) \quad \text{at } r = r_0, \quad \text{for } t > 0, \tag{1b}$$

$$\frac{\partial T}{\partial r} = \frac{h}{k}(T - T_\infty) \quad \text{at } r = R, \quad \text{for } t > 0, \tag{1c}$$

$$T = T(r) \quad \text{for } t = 0, \quad \text{in } r_0 < r < R, \tag{1d}$$

where k is the thermal conductivity, ρc_p is the volumetric heat capacity, $T_s(t)$ is the temperature at $r = r_0$, and $T(r)$ is the cylinder initial temperature between the inner and outer walls. The Crank–Nicholson (CN) method solves numerically the heat transfer model presented in Equation (1). This method, besides providing unconditional stability, offers second order accuracy $O(\Delta r^2, \Delta t^2)$ in both space and time [23,24]. Before finding the CN representation of Equation (1a), let us rewrite it as follows:

$$\frac{\partial^2 T}{\partial r^2} + \beta\frac{\partial T}{\partial r} = \frac{1}{\alpha}\frac{\partial T}{\partial t}, \tag{2}$$

where $\alpha = \dfrac{k}{\rho c_p}$ is the thermal diffusivity and $\beta = \left(\dfrac{1}{r} + \dfrac{1}{k}\dfrac{\partial k}{\partial r}\right)$ is an extra coefficient added to the equation when the thermal conductivity is assumed to vary with respect to r. Even though here we express Equation (2) in its CN form to have a more general approximation, for the inversion procedure, we supposed k, ρc_p, and h to be constant to avoid ill-conditioning in increasing the dimension of k.

Now, to find the finite difference equation as in the CN method, we substitute the following second order derivative approximations into Equation (2):

$$\frac{\partial T}{\partial t}(r_i, t_l) \approx \frac{T_i^{l+1} - T_i^l}{\Delta t}, \tag{3a}$$

$$\frac{\partial T}{\partial r}(r_i, t_l) \approx \frac{T_{i+1}^l - T_{i-1}^l}{2\Delta r}, \tag{3b}$$

$$\frac{\partial^2 T}{\partial r^2}(r_i, t_l) \approx \frac{T_{i+1}^l - 2T_i^l + T_{i-1}^l}{2\Delta r^2} + \frac{T_{i+1}^{l+1} - 2T_i^{l+1} + T_{i-1}^{l+1}}{2\Delta r^2}. \tag{3c}$$

After plugging Equation (3) into Equation (2), we obtain Equation (4), where $\lambda_i = \dfrac{\alpha_i \Delta t}{2\Delta r^2}$, $\Gamma_i = \dfrac{\beta_i \Delta r}{2}$. β_i is expressed as $\dfrac{1}{r_0 + \Delta r i} + \dfrac{1}{k_i}\dfrac{\partial k}{\partial r}(r_i)$. $\dfrac{\partial k}{\partial r}(r_i)$ is approximated by using second order forward and backward differences at the first and last points of the grid, respectively, while it is approximated by using center differences at the interior points:

$$\begin{gathered}\lambda_i T_{i-1}^{l+1} - (2\lambda_i + 1)\, T_i^{l+1} + \lambda_i T_{i+1}^{l+1} = \ldots \\ -\lambda_i\,(1 - \Gamma_i)\, T_{i-1}^l - (2\lambda_i - 1)\, T_i^l - \lambda_i\,(1 + \Gamma_i)\, T_{i+1}^l.\end{gathered} \tag{4}$$

Using Equation (4), we can set up a system of $n - 2$ linear equations that allow us to solve for the temperatures T_i, $i = 2, \ldots, n-2$ for t_{l+1}. The values T_1^l and T_n^l allow the incorporation of the boundary conditions (Equation (1b,c)) into the CN model by modifying Equation (4) for $i = 2$ and for $i = n - 1$

as indicated in Equations (5) and (6), respectively. In these two equations, l.b.c. and r.b.c. stand for a term added by the incorporation of the left and right boundary conditions, respectively:

$$\begin{aligned} -(2\lambda_2+1)\,T_2^{l+1}+\lambda_2 T_3^{l+1} &= \ldots \\ -\lambda_2(1-\Gamma_2)\,T_1^l-(2\lambda_2-1)\,T_2^l-\lambda_2(1+\Gamma_2)\,T_3^l-\lambda_2\underbrace{T_s(t_i)}_{\text{l.b.c.}}, & \end{aligned} \tag{5}$$

$$\begin{aligned} \underbrace{-\lambda_{n-1}\left(\frac{k_n}{3k_n+2\Delta rh}\right)}_{\text{r.b.c.}}T_{n-2}^{l+1}-\left(2\lambda_{n-1}+1+\underbrace{\lambda_{n-1}\frac{4k_n}{3k_n+2\Delta rh}}_{\text{r.b.c.}}\right)T_{n-1}^{l+1} &= \ldots \\ -\lambda_{n-1}(1-\Gamma_{n-1})\,T_{n-2}^l-(2\lambda_{n-1}-1)\,T_{n-1}^l-\lambda_{n-1}(1+\Gamma_{n-1})\,T_n^l \ldots & \\ -\lambda_{n-1}\underbrace{\frac{2\Delta rh}{2\Delta rh+3k_n}T_\infty}_{\text{r.b.c.}}. & \end{aligned} \tag{6}$$

For the sake of clarity, it is worth mentioning that Equation (3c) was discretized by using second order backward differences to estimate T_n at the boundary.

Additionally, Figure 1 gives some useful insights into the heat conduction problem described by Equation (1) in steady-state. Figure 1 shows the temperature at $r = R$, which is the cylinder face subjected to convection, against the heat transfer coefficient at time $t = 3596.4$ s (the average time at which the inspected bamboo culms reach steady state heat conduction). Since we assume the bamboo culms are subjected to free convection, in our simulations, the convection heat transfer coefficient ranges from 0 to 50 W/m^2·K. From Figure 1, one observes that the higher k is, the more linear the relationship between the outer temperature and h becomes. Observing Figure 1, we can roughly estimate that the thermal conductivity of bamboo samples and the heat transfer coefficient are around $k = 0.3$ W/m·K and $h = 25$ W/m^2·K since the temperatures obtained in the experiments oscillate around 38 °C. It is important to note that the heat conduction model was chosen to be more suitable for the temperature information we can access by the available instruments. Imposed thermal flux models are unfeasible for this direct problem since we have no available instruments to measure the input heat flow on the inner wall in our experimental set-up, and this heat flow is time variant and spatially uneven.

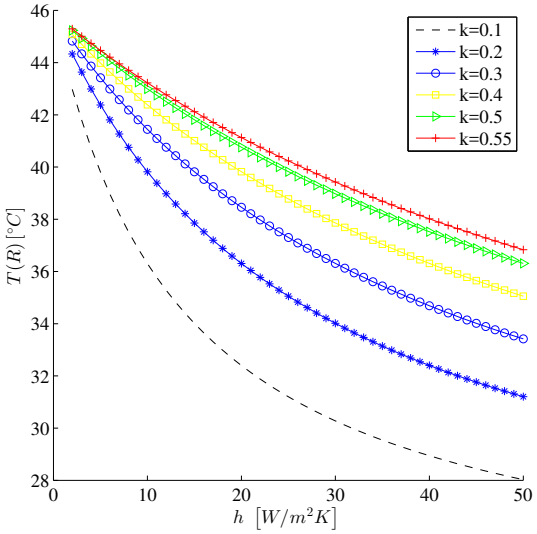

Figure 1. Steady state surface temperature on the cylinder's convex side against heat transfer coefficient for different values of thermal conductivity.

3. Inverse Problem Formulation

In this paper, we analyze the effects of bamboo preservation on bamboo's thermo-physical parameters. Consequently, we focus on the inverse problem of retrieving k, and ρc_p of a bamboo sample heated with an electric resistor. From Equation (2), one can also think of estimating h in which case we would cope with an *inverse problem* in which not only are the thermophysical properties of the material unknown but the boundary conditions as well. This problem, however, is not easily solved because of strong correlation between parameters and ill-conditioning. In Section 4, we show some disadvantages of including h in the estimation process.

Given $p = [k, \rho c_p]$ as vector of unknown parameters in Equation (1), we intend to estimate these quantities through nonlinear least-squares regression using the surface temperature evolution $T_{cam}(R, it_s)$ on the cylinder's convex side measured with an infrared camera, where $t_s = \frac{1}{30}$ is the sampling time, $i \in \{0, 1, 2, 3, 4, 5, 6, 7, ..., m\}$, and $T_s(it_s)$ is determined as:

$$\frac{1}{a_0} \sum_{j=0}^{j=1} b_j T_{res}(t_s(i-j)) + a_1 T_s(t_s(i-1)), \tag{7}$$

where $T_{res}(it_s)$ is the known temperature of a tubular resistor placed at $r = 0 < r_0$. Coefficients (a_j, b_j) represent the heat losses in the experimental platform that cannot be included explicitly in the heat diffusion equation. Section 5 explains the estimation of these parameters. Figure 2 shows the methodology used here to estimate these parameters [25]. The datasets are available to the interested readers upon request to the authors.

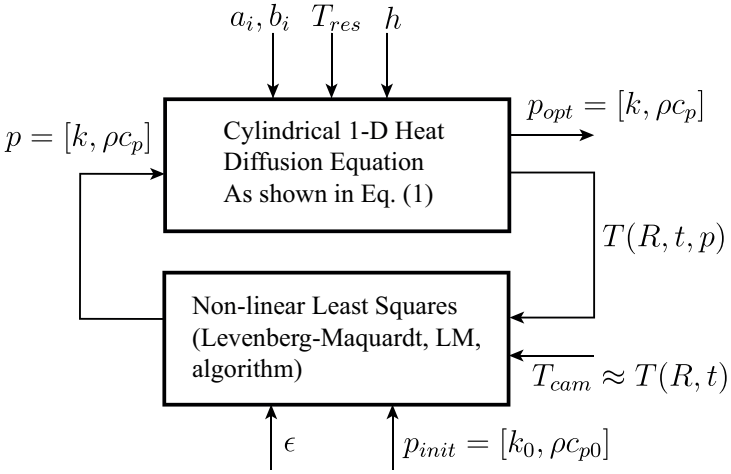

Figure 2. Methodology to address the Inverse Heat Conduction Problem (IHCP) presented above. Assuming a_i, b_i, T_{res}, and h as known. $T(R, t, p)$ is fitted to T_{cam} by varying p using the Levenberg–Maquardt (LM) algorithm. The algorithm stops and yields p_{opt} when one of these criteria is met (i) $max|J^T W(T_{cam} - T(p))| < \epsilon$ (ii) $max|\frac{\Delta p_i}{p_i}| < \epsilon$ (iii) $\frac{\chi^2}{m-n+1} < \epsilon$. The LM algorithm is highly sensible to p_{init} especially when the IHCP is nonlinear in the parameters, thus it must be carefully chosen.

Measuring an estimate's accuracy is difficult, above all when there is little to no clue about the true values. Nonetheless, we can measure the consistency and robustness of a solution with respect to unexplained variability in the data through the asymptotical standard parameter error σ_p defined in Equation (8). This variability may be a consequence of something simple such as instrumental noise, or parameter correlation, or something more complex like the lack of completeness in the model that disregards some facts about the true nature of the problem [26]:

$$\sigma_p = \sqrt{diag\left(\left[J^T W J\right]^{-1}\right)}, \tag{8}$$

where J is the sensitivity matrix, W is diagonal matrix whose diagonal is $diag(W) = \sigma_T^2 = \frac{1}{m-n+1}(T-\hat{T}(p_{fit}))^T(T-\hat{T}(p_{fit}))$, and n is the parameter vector length. There are three important facts to highlight about this metric. First, very noisy data increase the value of σ_p. Second, highly correlated parameters certainly increase σ_p, meaning that any change in one parameter results in changes in the other parameters. In our case, the convective coefficient h is a difficult parameter to control and know beforehand since it varies depending on the materials surface and the environmental conditions. Third, ill-conditioning of an IHCP can be noticed through σ_p, as it depends on J, small eigenvalues of J causes the standard error to rise drastically [26].

Additionally, sensitivity coefficients allow us to characterize the IHCP as either linear or nonlinear in the parameters. Non-linearity in the parameters makes any IHCP sensitive to measurement errors [27]. Figure 3a displays the relative sensitive coefficients for our inverse heat conduction scenario. Here, we show that, as h increases, not only does J_h change, implying that it depends on h and so the IHCP is nonlinear with respect to h, but h variation also causes J_k and $J_{\rho c_p}$ to vary, thus demonstrating correlation between the parameters. Likewise, the variation of k and ρc_p also introduces an effect on the other relative sensitivity coefficients. Figure 3a also shows that the volumetric heat capacity ρc_p strongly affects the transitory state of the heat conduction. In contrast, h and k most influence the temperature behavior at the steady state. In estimating parameters through temperature measurements, the sensor position is also fundamental; Figure 3b shows that J_r varies with position. For instance, at $r = R$, where we have located our sensor (with no possibility of relocation since we intend to perform a non-destructive test), temperature response is lagged and attenuated, making it harder to estimate parameters by using these temperature measurements. As our IHCP also exhibits correlation among parameters and nonlinearity, the problem of estimating thermo-physical properties of materials, in this scenario, is challenging.

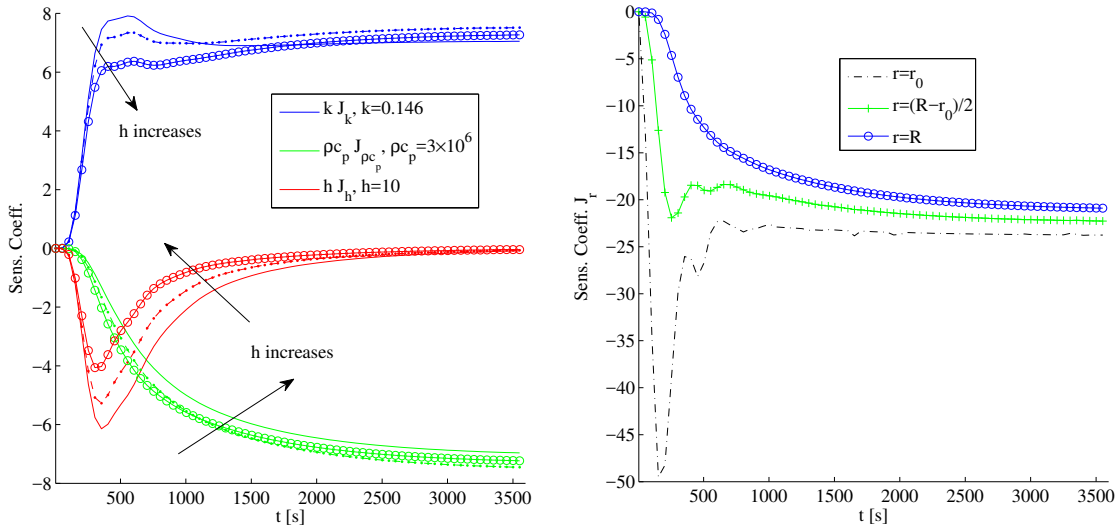

(**a**) (**b**)

Figure 3. Relative sensitivity coefficients. (**a**) J_k, J_h and $J_{\rho c_p}$; and (**b**) J_r are the first derivatives of the temperature with respect to k, h, ρc_p, and r (position within the cylinder).

An additional fact to point out is that a substantial difference in the range of the parameters to estimate makes the LM algorithm very sensitive to noise, preventing it from converging, as volumetric heat capacity and thermal conductivity take values proportional to 10^6 and 10^{-1} for bamboo, respectively, we decided to optimize the volumetric heat capacity in the range of 2–10, but the model

internally multiplies it by 10^6. This approach increases the probability of convergence and produces better Jacobean matrices.

4. Estimation of Thermo-Physical Properties of Bamboo Using Synthetic Data with Additive White Gaussian Noise

In order to gain insight into the estimation of the thermo-physical properties of a material and its surrounding medium from transient temperature measurements, we generate synthetic data by solving the heat diffusion equation explained in Section 2 through the Crank–Nicholson method for a known set of parameters $p_t = (k, \rho c_p, h)$. Even though this experiment uses data from the solution of the direct model, it allows us to observe how the LM regression algorithm performs under different conditions such as noisy data and random initialization. The noisy data was generated by adding additive white Gaussian noise (with standard deviations σ of 0.1) to the data. Random initialization, on the other hand, was performed by randomly choosing parameters in the set of initial random guesses $S = \{p_{init} = (k, \rho c_p, h) \mid 0.4p_{t,1} < k < 1.6p_{t,1},\ 0.4p_{t,3} < \rho c_p < 1.6p_{t,3},\ 0.4p_{t,2} < h < 1.6p_{t,2}\}$. It is necessary to take into account that as k, ρc_p, and h form fractions in the heat diffusion model, a scaled version of them will always allow a perfect curve-fitting even if the parameters are not the ones we used to calculate the numerical solution. That is why it is preferable to have an initial guess whose components (or individual parameters) do not have a scaling factor in common. For instance, if p_t is the actual value toward which the LM algorithm must converge, p_{init} cannot be $1.2p_t$. Instead, we should multiply every individual component by a different factor i.e., $p_{init} = (1.2p_{t,1}, 0.9p_{t,1}, 0.6p_{t,1})$. These kinds of initial guesses prevent us from obtaining, at least in the first iteration, a valid solution but far from the actual one.

Even though we carefully choose the initial guesses as described above, when optimizing the three parameters at once, the results are not satisfactory. For any initial guess, the algorithm finds a convergence point that lies on a three-dimensional line as shown in Figure 4. Those optimal points are all equivalent and are in predefined boundaries, so they all could be a possible solution. However, they differ from the true parameter values. This undesirable behavior that does not allow the algorithm to be robust against initial conditions is a consequence of highly correlated parameters. Here, we deal with the problem by reducing the complexity of the inverse heat problem by optimizing over a two-dimensional space, where the parameter vector is now $p = (k, \rho c_p)$ while h is assumed constant. This action improves the algorithm robustness against initial conditions, reducing uncertainty in the estimation quantified through the asymptotical standard error σ_p.

Table 1a,b show the results of the curve-fitting scenario aforementioned. It is worth recalling that only two parameters k and ρc_p are optimized, while h is assumed known. For this case, we try to fit a noisy temperature curve with parameters $k = 0.146$ W/m·K, $\rho c_p = 3.5 \times 10^6$ J/m^3·K, and $h = 10$ W/m^2·K. In a realistic scenario, the value of h would be difficult to find. That is why we assume different values for h keeping them in the natural convection range from 2 to 25 J/m^3·K, and then observe how these blindly chosen h values affect the estimation by using the relative error. Table 1a shows these results. $\bar{p_{fit}}$ is the average convergence value that results from initializing the LM algorithm with 50 initial guesses obtained as explained in previous paragraphs. As seen in the table, the standard deviation of these estimates is of order 10^{-8} approximately, which shows that the algorithm responds well to initial conditions' variability. We see as well that when h is chosen mistakenly, the relative errors are very high; they can reach values up to 150%, which is unacceptable. Nonetheless, Table 1b shows that dividing k into ρc_p, the LM algorithm accurately retrieves thermal diffusivity (α_{fit}) with an error up to 0.395% for any value of h. As a consequence, estimating the thermal diffusivity of the material makes the LM algorithm less sensitive to the unawareness of h.

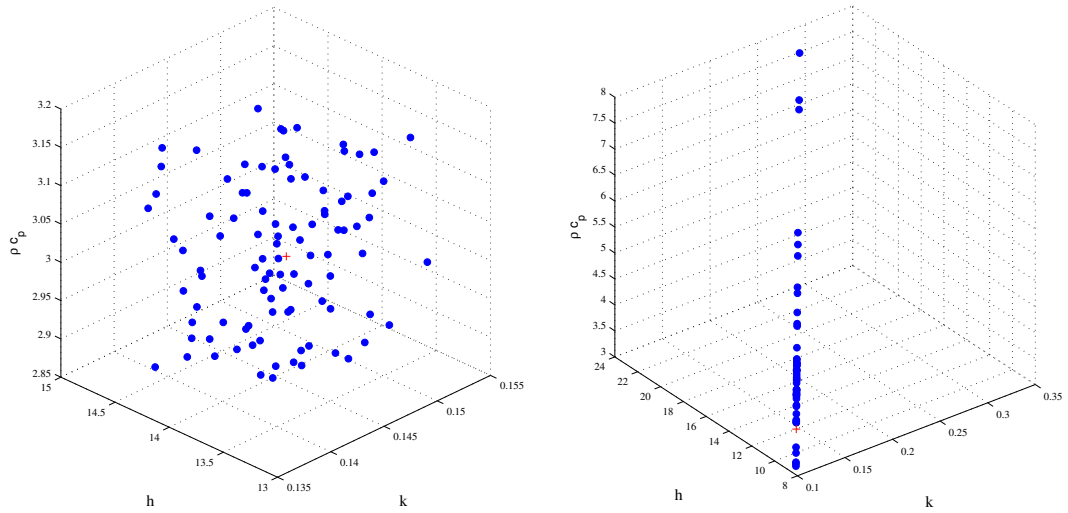

Figure 4. Initial guesses (**a**) and convergence points (**b**) for the LM algorithm in a three-dimensional parameter space.

Table 1. Results of parameter estimation with synthetic data for (**a**) p_t and (**b**) α_t obtained from p_t. One hundred random initial guesses were used to estimate $\bar{p_{fit}}$, which is the average of the optimal estimates. The two columns in p_t refer to k, ρc_p, respectively.

(**a**)								
h	p_t		$\bar{p_{fit}}$		$\sigma_{fit} \times 10^{-8}$		$\frac{\lvert p_t - \bar{p_{fit}} \rvert}{p_t} \times 100$	
7	[0.146	3.500]	[0.102	2.437]	[0.8366	128.51]	[30.07	30.35]
10	[0.146	3.500]	[0.145	3.482]	[4.4487	514.92]	[0.112	0.506]
25	[0.146	3.500]	[0.364	8.775]	[2.7828	409.99]	[149.7	148.7]

(**b**)				
h	α_t	$\bar{\alpha_{fit}} \times 10^{-8}$	σ_{fit}	$\frac{\lvert \alpha_t - \bar{\alpha_{fit}} \rvert}{\alpha_t} \times 100$
7	0.0417	0.0419	1.883×10^{-8}	0.395
10	0.0417	0.0419	7.301×10^{-8}	0.395
25	0.0417	0.0419	1.654×10^{-8}	0.395

5. Experimental Set-Up

5.1. Guadua's Samples Preparation

In this work, we tested 10 cylindrical pieces of Guadua a.k. that were divided into 20 pieces by splitting each into two parts as shown in Figure 5. The average height of the samples is of 15.81 ± 0.24 cm, the average thickness is of 7.83 ± 0.78 mm, and the average outer diameter is of 6.94 ± 0.41 cm. Half of the inspected samples underwent a preservation process in which the samples were submerged in a mixture of 16 L of water with 0.4 kg of boric acid and boron at 5% of concentration. The mixture was kept at 60 °C for better and fast bamboo preservation during 24 h. When bamboo preservation ended, the samples were dried at 100 °C for 24 h, resulting in an average humidity of $11.86 \pm 1.6\%$.

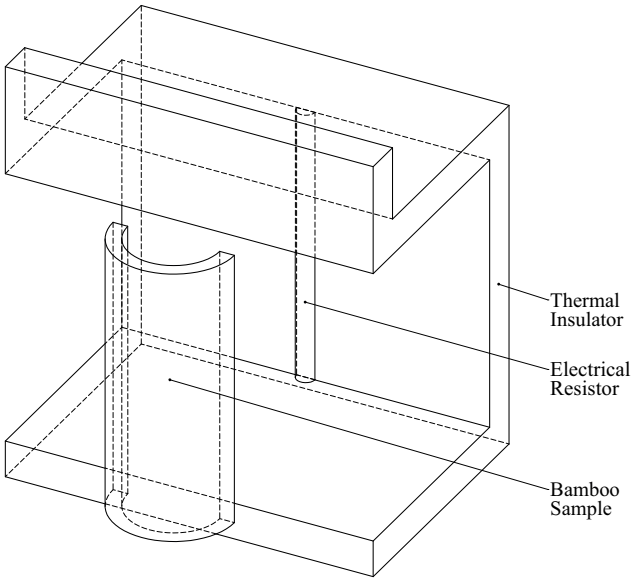

Figure 5. Experimental measurement platform.

5.2. Thermal Data Acquisition

The temperature measurements were performed using the experimental platform that is shown in Figure 5. The thermal insulator, 'Isoboard FC' material, has a thermal conductivity of 0.085 W/m·K. The heat source is a 60 W-electric resistor that we control at 90 °C using a Proportional–Integral–Derivative (PID) controller and a J type thermocouple. An IR camera FLIR T360 (FLIR Systems, Wilsonville, Oregon, United States) remotely measures the temperature on the convex face of the cylindrical bamboo sample. This camera has an FPA (Focal Plane Array) with size of 320 × 240, a field of view of 25 × 19°, a thermal sensibility of 0.06 °C, and a spectral range from 7.5 μm to 13 μm.

Figure 6 presents the general scheme of the video acquisition. In the acquisition scheme, the heat source is energized using a variac to reduce the power supplied to the resistance since the controlled response has a high overshoot. Then, we decide to reduce the power from 60 W to 10 W.

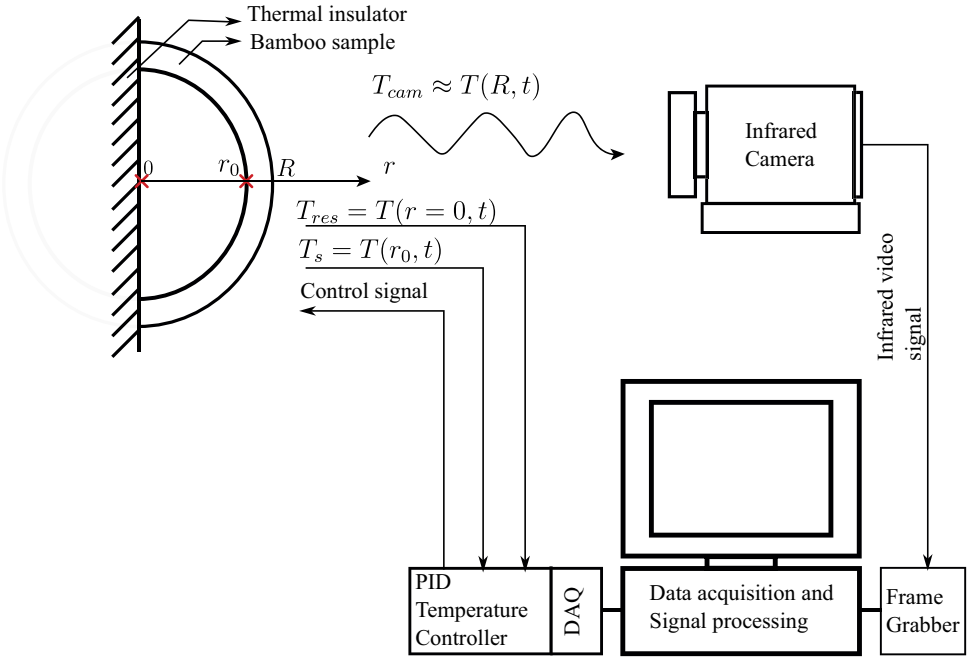

Figure 6. Scheme of temperature acquisition.

The IR camera records external temperature variations of the sample produced by the heat source. The calibration process transforms image gray levels acquired with the frame-grabber into temperature values that range from 18 °C to 100 °C. The transformation function is a fourth degree polynomial that provides an error of 0.2 °C in the conversion.

A region of interest (ROI) that contains the bamboo sample is selected from the 720 × 480 images provided by the frame grabber. This region is chosen to have its emissivity unaffected by the viewing angle since the camera's optical axis is located to be, to the best of our ability, perpendicular to the selected region. Each experiment lasts one hour, in which the bamboo sample temperature T_{cam} is taken from one pixel in the ROI and recorded with a sampling frequency of 30 fps. Then, this signal is decimated to take one frame every 5 s and reduce the memory space. This sub-sampled signal (T_{cam}) along with the resistance temperature (T_{res}) are the inputs to the inversion algorithm that estimates parameters k and ρc_p. Figure 7 shows an example of these temperature inputs taken with a emmisivity of 0.96 for the bambbo surface and a reflected temperature of 20 °C set in the camera.

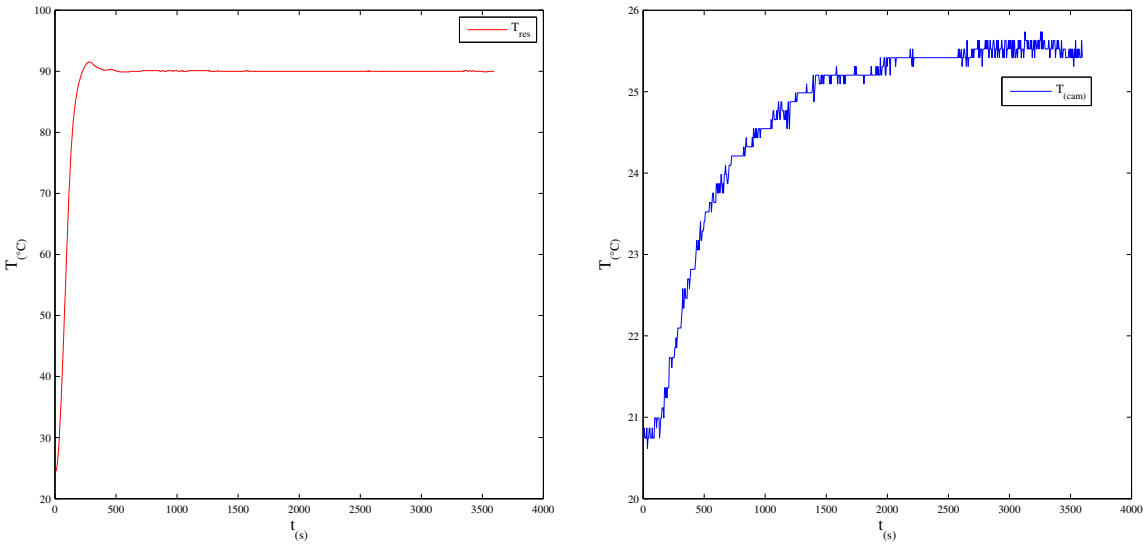

(**a**) (**b**)

Figure 7. Examples of temperature curves in (**a**) the electrical resistence T_{res} and (**b**) T_{cam} the external side of the bamboo sample.

The internal temperature of the bamboo sample is measured with a K type thermocouple and a FLUKE 179 multimeter (Fluke Electronics, Everett, Washington, United States). There is a decrease of temperature in the internal side of the bamboo sample, with respect to T_{res}. Therefore, we estimate a bank of eight Infinite Impulse Response (IIR) filters to account for this phenomenon. Matlab's System Identication Toolbox calculates the parameters of each filter $H(z)$ represented by Equation (9). R^2 validates the fitting of each model $H(z)$, obtaining values that range from 0.96 to 0.99:

$$H(z) = \frac{b_0 + b_1 \cdot z^{-1}}{1 + a_1 \cdot z^{-1}}. \tag{9}$$

6. Estimation of Thermo-Physical Properties of Bamboo Using Experimental Data

Estimating thermo-physical properties of bamboo can be complicated, particularly when done in a non-destructive way. Bamboo's tissue is inhomogeneous; it varies along and across the culm. Most of the studies [10,28,29] that estimate thermal properties of bamboo both along and across the culm take small pieces of bamboo culms since the analysis equipment imposes such specific geometries on the specimens to be analyzed. Even though these works provide insight into the thermal properties of bamboo, they lack practical use when inspecting numerous samples whose geometries are mostly cylindrical.

Here, we address the problem of estimating thermal conductivity, volumetric heat capacity, and convective heat transfer coefficient of bamboo samples, which are approximately half a cylinder, from data obtained as explained in Section 5. The direct model assumes no interactions in z and ϕ directions and constant properties radially to reduce complexity in the inverse procedure. Therefore, our experiments yield average values of k, ρc_p, and h.

As mentioned in Section 4, estimating k, ρc_p, and h is challenging not only for the nonlinearity of the IHCP, but for the correlation among the three parameters. As a result, we optimized over the parameter space defined by k and ρc_p while h is assumed known. Removing h from the optimization parameters diminishes the correlation between k and ρc_p from 1 to 0.6 ± 0.15. This allows the LM algorithm to have more consistent results in the sense that variations of 5% around an initial guess produce variations of 0.1% around the convergence point of the initial guess, which is a desirable behavior according to [26].

Table 2 shows the average estimates of ten bamboo samples subjected to preservation and another ten left untreated (as exposed in Section 5). Although on average we find the estimates to be consistent with the measurements performed by [9,10,29], bamboo itself poses a big challenge because its properties depend on its species, porosity, density, vessel distribution among others. In addition, it is worth noting that in general it is difficult to make a fair comparison since most of the works in this area use different techniques and assumptions to measure the thermal properties of bamboo.

Table 2. Average parameter estimates (obtained by using the LM algorithm) for unpreserved and preserved bamboo samples. Ten bamboo samples were used to estimate $p\bar{_{fit}}$ which is the average of the optimal estimates of each bamboo sample. The two columns in both $p\bar{_{fit}}$ and $\bar{\sigma_p}$ refer to k, ρc_p, respectively.

Bamboo Category	h [W/m^2·K]	$p\bar{_{fit}}$ [W/m·K J/m^3·K]		$\bar{\sigma_p}$		R^2
unpreserved	15	[0.109	4.200×10^6]	[0.0010	0.1476]	0.98
	25	[0.154	6.744×10^6]	[0.0004	0.0644]	0.99
	35	[0.215	9.020×10^6]	[0.0006	0.0874]	0.99
preserved	15	[0.111	4.274×10^6]	[0.0008	0.1148]	0.99
	25	[0.168	7.175×10^6]	[0.0005	0.0738]	0.99
	35	[0.233	9.100×10^6]	[0.0008	0.1162]	0.98

Table 2 also shows that, although the variation of h causes great changes in the estimated parameters (k and ρc_p), the standard errors are small in magnitude; the least standard error is reached when h equals 25, however. Figure 8 shows the curves of the estimates against the bamboo sample number. These curves permit us to visualize that, for values of h less than 25, the estimation of k tends to the lower bound in the optimization parameter space (OPS). By contrast, when h is greater than 25, some values ρc_p tend to the upper bounds in the OPS. This effect is undesirable since it implies that the optimization action of the LM algorithm is being saturated, thus converging to a optimal value that is unnatural within the defined bounds. As a result, we consider that values of the parameters that converge within the bounds are better than those that lie over the lower and upper bounds; in this case, the best results are achieved when $h = 25$. Here, as done in Section 4, we also remove the scaling effect of h by dividing the curves in Figure 8 to obtain the thermal diffusivity of the bamboo samples as shown in Figure 9. In this figure, we can see that, for every value of h, the thermal diffusivity of the samples tend to be the same except for the points that converge to lower limits of the thermal conductivity boundaries. Figure 10a accounts for the goodness of fit of the proposed approach for a chosen experimental temperature curve. σ_y is the standard error of the fit that exhibits higher values at the beginning of the heating. This bias is due to the over estimation of the prediction model. However, σ_y is still low. The overestimated temperature data reflects in the histogram of residuals showed in Figure 10a. Even though this distribution is biased toward right, it is still a normal distribution, which is a desirable property that guarantees no systematic error.

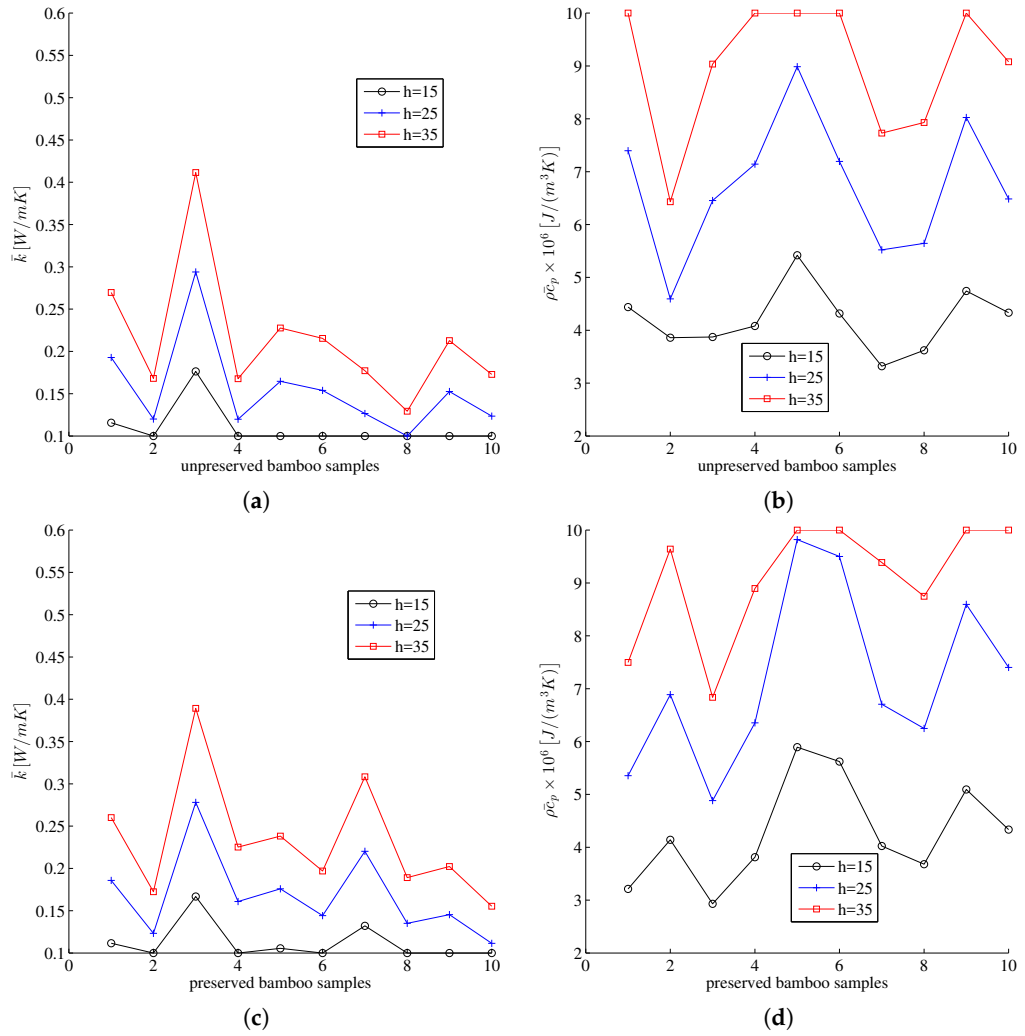

Figure 8. k and ρc_p estimates for unpreserved (**a**) and (**b**) and preserved (**c**) and (**d**) bamboo samples as the convective coefficient of air h varies.

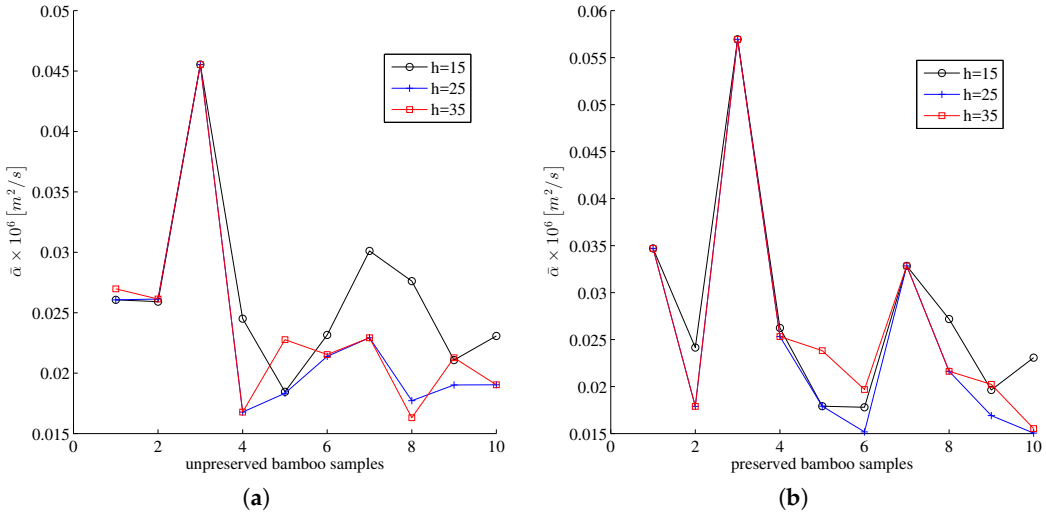

Figure 9. Thermal diffusivity estimates for unpreserved (**a**) and preserved (**b**) bamboo samples. The curves were obtained by dividing thermal conductivity and volumetric heat capacity curves displayed in Figure 3.

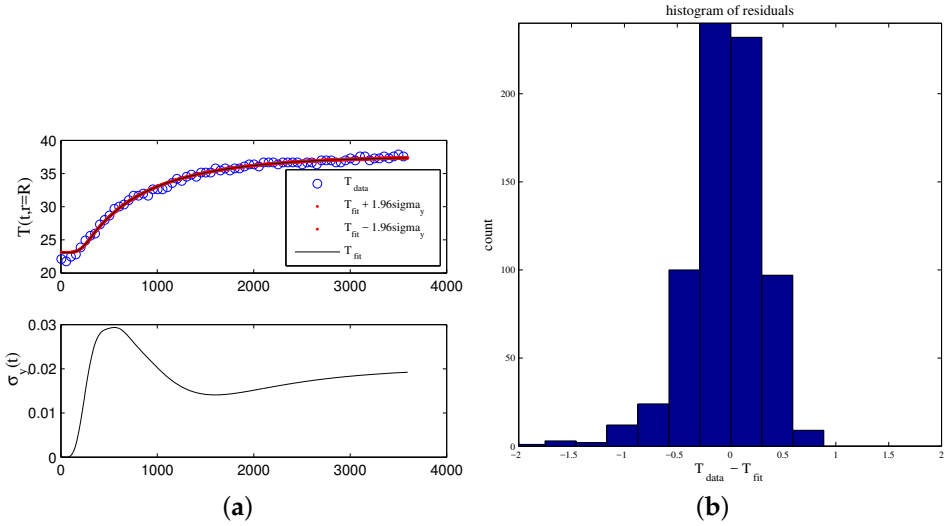

Figure 10. (**a**) top: temperature data and fitted-temperature data, with confidence intervals of 96% (**a**) bottom: standard error of the fit, $\sigma_{y(t)}$; (**b**) histogram of curve-fitting residuals.

In this work, furthermore, the bamboo preservation process is based on a diffusion treatment with a combination of borax and boric acid. In this process, molecules of the preservative migrate through a porous medium, bamboo [30]. According to our experiments, the differences between thermal properties of preserved and non-preserved bamboo samples are not significant to conclude about the quality of preservation based on thermal parameters. A reason for this result is that the temperature evolution on the external face of the bamboo is not sensitive enough to variations of density and porosity generated by treatment process. Furthermore, bamboo is a non-homogeneous material and is seldom totally saturated with water when treated and dried causing a non-uniform distribution of preservant across the specimen. In a similar work carried out on laminated veneer lumber, the authors have found that thermo-physical properties such as the thermal conductivity k and volumetric heat capacity ρc_p of materials may vary after preservation process [28], although they manifest that further studies have to be done to corroborate whether these variations are a consequence of chemical interactions of preservatives with the wood or with the adhesives that join the wood laminates.

7. Conclusions

In this paper, the estimates of thermal properties k and ρc_p in Guadua a.k. specimens are obtained by an inverse method from temperature data. The transient temperature data were acquired by using non-invasive active IT in transmission mode (i.e., the camera and the heat source are at opposite faces of the sample). Tests were conducted on both preserved and unpreserved Guadua a.k. culms. One of the great advantages is the determination of thermo-physical properties in a non-destructive and straightforward experiment, without cutting or preparing the sample into specific geometries or shapes.

In spite of the nonlinearity and high correlation in the parameters of this IHCP, we found that, according to the asymptotical parameter and fit standard errors σ_p and σ_y, the estimates of k and ρc_p across different bamboo specimens are consistent and robust with respect to variations in the initial conditions. Setting h in values less than 15 $W/m^2 \cdot K$ units makes the estimates of k and ρc_p converge to the lower bound of optimization range. Nonetheless, the estimation of the thermal diffusivity α instead of k and ρc_p separately makes the LM algorithm less sensitive to the unawareness of h.

Finding a sole value for thermal conductivity and volumetric heat capacity for Guadua a.k. is not straightforward, as thermal properties may vary for numerous reasons, moisture content, density, inner vessel distribution, etc. Measurements of thermal conductivity on bamboo board have shown that

this parameter ranges from 0.121–0.384 W/m·K computed by using steady-state guarded hot-plate [9]. Ref. [10] reports that the values for k and ρc_p are approximately 0.33 W/m·K and 3×10^6 J/m^3·K when computed using photoacoustic data. What is certain about these estimations is that they are in the range of thermal insulators (0.04–0.9 W/m·K) [31].

Even though the proposed approach yields estimated values of k and ρc_p that are h-dependent, the estimated values lie in the range of thermal insulators as well. In addition, the volumetric heat capacity is comparable with the values reported in [10]. It is worth noting that estimated thermal diffusivity presents little to no dependency on h. The estimated values, nonetheless, are less than those of woods, because of bamboo's higher capacity to store heat as shown in [32].

Our tests show that the differences between thermal properties of preserved and non-preserved bamboo samples are not significant to make conclusions about the penetration of preservatives into the bamboo samples.

We believe that the proposed inversion approach can serve as a solid starting point for further infrared nondestructive inspections of Guadua a.k. specimens to estimate parameters such as defect depth and thickness in green composites.

Acknowledgments: The authors greatly appreciate the financial support received by COLCIENCIAS in the research project: Estimation of boron concentration in bamboo samples through infrared thermography. They also thank the support received with the preparation of bamboo samples and construction of experimental set-up from Centro de Automatización de Procesos (CAP) at Pontificia Universidad Javeriana in Cali. We also thank Gilberto González Gómez, assistant professor in the Department of Chemical and Biochemical Engineering at Instituto Tecnológico de Celaya in Mexico for his valuable help on the modeling of the heat conduction problem.

Author Contributions: J.F.F.-O., J.E.O.-B. and H.D.B.-R. wrote this paper together.

Conflicts of Interest: The authors declare no conflict of interest.

Abbreviations

The following abbreviations are used in this manuscript:

IHCP	Inverse heat conduction problem
PLA	Poly lactic acid
BMB	Bamboo mat board
IT	Infrared thermography
FMTW	Frequency modulated wave imaging
CN	Crank–Nicholson
FPA	Focal plane array
ROI	Region of interest
OPS	Optimization parameter space

References

1. International Network for Bamboo and Rattan (INBAR). *Bamboo in Construction: An Introduction*; Technical Report 16; INBAR: Beijing, China, 1998.
2. Londono, X.; Camayo, G.C.; Riano, N.M.; López, Y. Characterization of the anatomy of guadua angustifolia. *Bamboo Sci. Cult. J. Am. Bamboo Soc.* **2002**, *16*, 18–31.
3. Dixon, P.G.; Gibson, L.J. The structure and mechanics of Moso bamboo material. *J. R. Soc. Interface* **2014**, *11*, 20140321.
4. Correal, J.; Echeverry, J.; Ramirez, F.; Yamin, L. Experimental evaluation of physical and mechanical properties of Glued Laminated Guadua angustifolia Kunth. *Constr. Buid. Mater.* **2014**, *73*, 105–112.
5. Correal, J.; Lopez, L. Chapter Mechanical Properties of Colombian Glued Laminated Bamboo. In *Modern Bamboo Struct*; CRC Press Taylor & Francis Group: London, UK, 2008; pp. 121–128.
6. Chung, K.; Yu, W. Mechanical properties of structural bamboo for bamboo scaffoldings. *Eng. Struct.* **2002**, *24*, 429–442.
7. Takagi, H.; Kusano, S.K.; Ousaka, A. Thermal conductivity of PLA-bambbo fiber composites. *Adv. Compos. Mater.* **2007**, *16*, 377–384.

8. Mounika, M.; Rmaniah, K.; Prasad, A.R.; Rao, K.M.; Reddy, K.H.C. Thermal conductivity characterization of bamboo fiber reinforced polyester composite. *J. Mater. Environ. Sci.* **2012**, *3*, 1109–1116.
9. Kiran, M.; Nandanwar, A.; Venugopal, M.; Rajulu, K. Effect of density on thermal conductivity of bamboo mat board. *Int. J. Agric. For.* **2012**, *2*, 257–261.
10. Delgado, F.G.; Hernández, D.C.; Morales, C.M. Comportamiento de los parámetros termofísicos de la Guadua angustifolia-Kunth medidos con la técnica fotoacústica. *Rev. Colomb. Física* **2012**, *44*, 3491–3496.
11. Maldague, X. *Theory and Practice of Infrared Technology for Nondestructive Testing*; Wiley: Hoboken, NJ, USA, 2001.
12. Vavilov, V. Thermal NDT: Historical milestones, state-of-the-art and trends. *Quant. InfraRed Thermogr. J.* **2014**, *11*, 66–83.
13. López, G.; Basterra, L.A.; Acuña, L. Estimation of wood density using infrared thermography. *Constr. Build. Mater.* **2013**, *42*, 29–32.
14. Lundgren, N.; Hagman, O.; Johansson, J. Predicting moisture content and density distribution of Scots pine by microwave scanning of sawn timber II: Evaluation of models generated on a pixel level. *J. Wood Sci.* **2006**, *52*, 39–43.
15. Wyckhuyse, A.; Maldague, X. A study of wood inspection by infrared thermography, Part I: Wood pole inspection by infrared thermography. *Res. Nondestr. Eval.* **2011**, *13*, 1–12.
16. Wyckhuyse, A.; Maldague, X. A study of wood inspection by infrared thermography, Part II: Thermography for wood defects detection. *Res. Nondestr. Eval.* **2011**, *13*, 13–22.
17. Bucur, V. Thermal Imaging. In *Non-Destructive Characterization and Imaging of Wood*; Springer: Berlin/Heidelberg, Germany, 2003; pp. 75–122.
18. Smita, C.; Suneet, T.; Chatterjee, K.; Singh, S.; Sudhakar, P. Bamboo-glue interface thermography for non-destructive testing. *J. Bamboo Rattan* **2009**, *8*, 143–148.
19. Bendada, A.; Maillet, D.; Batsale, J.; Degiovanni, A. Reconstruction of a non uniform interface thermal resistance by Inverse heat conduction. *Inverse Probl. Eng.* **1998**, *6*, 79–123.
20. Santana, F.; Nunes, R. Infrared thermography applied to the quantitative determination of spatial and thermophysical parameters of hidden included objects. *Appl. Therm. Eng.* **2007**, *27*, 2378–2384.
21. Da Fonseca, H.M.; Orlande, H.R.B.; Fudym, O.; Sepúlveda, F. A statistical inversion approach for local thermal diffusivity and heat flux simultaneous estimation. *Quant. InfraRed Thermogr. J.* **2014**, *11*, 170–189.
22. Correal, J.; Ramirez, F. Adhesive bond performance in glue line shear and bending for glued laminated Guadua bamboo. *J. Trop. For. Sci.* **2010**, *22*, 433–439.
23. Glyn, J. *Advanced Modern Engineering Mathematics*; Prentice Hall: Upper Saddle River, NJ, USA, 2011.
24. Canale, R.P.; Chapra, S.C. *Numerical Methods for Engineers*; Mc Graw Hill: New York, NY, USA, 2010.
25. Github Code Repository. Available online: https://github.com/hbenitez/FlorezBenitez2017Bamboo (accessed on 28 November 2017).
26. Gavin, H.P. *The Levenberg-Marquardt Method for Nonlinear Least Squares Curve-Fitting Problems*; Duke University: Durham, NC, USA, 2011; pp. 1–15.
27. Beck, J.V. *Inverse Heat Conduction: Ill-Posed Problems*; John Wiley & Sons: Hoboken, NJ, UAS, 1985.
28. Kol, H.Ş.; Altun, S. Effect of some chemicals on thermal conductivity of impregnated laminated veneer lumbers bonded with poly (vinyl acetate) and melamine–formaldehyde adhesives. *Dry. Technol.* **2009**, *27*, 1010–1016.
29. Huang, P.; Chang, W.S.; Shea, A.; Ansell, M.P.; Lawrence, M. Non-Homogeneous Thermal Properties of Bamboo. In *Materials and Joints in Timber Structures*; Springer: Dordrecht, The Netherlands, 2014; pp. 657–664.
30. Williams, L. Diffusion Treatment of Wood–An American Perspective. In *the Chemistry of Wood Preservation*; Woodhead Publishing Limited: Sawston, UK, 2005; pp. 35–52.
31. Çengel, Y.A.; Ghajar, A.J. *Heat and Mass Transfer: Fundamentals & Applications*; McGraw-Hill: New York, NY, USA, 2011.
32. Mena, J.; Vera, S.; Correal, J.; López, M. Assessment of fire reaction and fire resistance of Guadua angustifolia kunth bamboo. *Constr. Buid. Mater.* **2012**, *27*, 60–65.